Published in final edited form as:
*Neuroimage*. 2012 April 15; 60(3): 1622–1629. doi:10.1016/j.neuroimage.2012.01.075.

# MRI hippocampal and entorhinal cortex mapping in predicting conversion to Alzheimer's disease

**D. P. Devanand, M.D.**[1], **Ravi Bansal, Ph.D.**[2], **Jun Liu, Ph.D.**[2], **Xuejun Hao, Ph.D.**, **Gnanavalli Pradhaban, M.B.B.S.**[1], and **Bradley S. Peterson, M.D.**[2]

[1]Division of Geriatric Psychiatry, New York State Psychiatric Institute, College of Physicians and Surgeons, Columbia University, New York.

[2]Division of Child Psychiatry, New York State Psychiatric Institute, College of Physicians and Surgeons, Columbia University, New York.

## Abstract

**Objective—**Using MRI surface morphometry mapping, to evaluate local deformations of the hippocampus, parahippocampal gyrus, and entorhinal cortex in predicting conversion from mild cognitive impairment (MCI) to Alzheimer's disease (AD).

**Methods—**Baseline brain MRI with surface morphological analysis was performed in 130 outpatients with MCI, broadly defined, and 61 healthy controls followed for an average of 4 years in a single site study.

**Results—**Patients with MCI differed from controls in several regions of the hippocampus and entorhinal cortex, and to a lesser extent in the parahippocampal gyrus. In the MCI sample, Cox regression models were conducted for time to conversion comparing converters to AD (n=31) and non-converters (n=99), controlling for age, sex and education. Converters showed greater atrophy in the head of the hippocampus, predominantly in the CA1 region and subiculum, and in the entorhinal cortex, especially in the anterior-inferior pole bilaterally. When distances of specific points representing localized inward deformation were entered together with the corresponding hippocampal or entorhinal cortex volume in the same Cox regression model, the distances remained highly significant whereas the volumes of the corresponding structures were either marginally significant or not significant. Inclusion of cognitive or memory measures or apolipoprotein E ε4 genotype as covariates, or restricting the sample to patients with amnestic MCI (24 converters and 81 non-converters) did not materially change the findings. In the 3-year follow-up sample of patients with MCI, logistic regression analyses using the same measures and covariates yielded similar results.

**Interpretation—**These findings indicate selective early involvement of the CA1 and subiculum regions of the hippocampus and provide new information on early anterior pole involvement in the entorhinal cortex in incipient AD. Fine-grained surface morphometry of medial temporal lobe structures may be superior to volumetric assessment in predicting conversion to AD in patients clinically diagnosed with MCI.



Corresponding author: D.P. Devanand, M.D. 1051 Riverside Drive, Unit 126, New York, NY 10032. Tel 212-543-5612, Fax 212-543-5854. dpd3@columbia.edu.

**Keywords**

MRI; hippocampus; entorhinal cortex; surface mapping; mild cognitive impairment; Alzheimer's disease

## INTRODUCTION

The medial temporal lobe, which includes the hippocampus and entorhinal cortex, atrophies early in Alzheimer's disease (AD) (de Leon et al., 2004, Jack et al., 2010). In patients with mild cognitive impairment (MCI), a condition that is often transitional to AD (Petersen et al., 2001), hippocampal and entorhinal cortex volumes lie between values in controls and AD (De Santi et al., 2001). In patients with MCI, hippocampal and entorhinal cortex atrophy, measured by reductions in overall volumes of these structures, show moderate to strong associations with conversion to AD (Devanand et al., 2007, Killiany et al., 2002, Stoub et al., 2005). Differing hippocampal subregions, however, have differing computational and information processing functions that may be specifically altered in MCI and AD. Therefore, measures of overall volumes of these structures may not be sufficiently sensitive to detect atrophy early in the course of illness, particularly if subnuclei within these structures have opposing effects of local increases and decreases in volume. Therefore, a regionally-specific shape analysis may be more powerful than conventional volumetric analysis to assess atrophy in hippocampal subregions in normal aging, MCI, and AD (Apostolova et al., 2006; Burggren et al., 2008; Csernansky et al., 2005).

Abnormalities in local volumes within these structures can be computed and compared using advanced image processing techniques, and several have been proposed that use geometric representations of morphological surfaces to detect small, localized changes in shape, surface area or volume (Csernansky et al., 2005, Peterson et al., 2007; Peterson et al., 2010, Qiu et al., 2009; Kim et al., 2005; Styner et al., 2006). Most of these methods describe morphology of a structure using global descriptors, which are subsequently compared between groups to localize changes in shape or volumes in these structures. Using these techniques, prior studies have shown that hippocampal deformation is pronounced in the CA1 region and the subiculum in AD, but less so in MCI and least in healthy comparison subjects (Tepest et al., 2008, Wang et al., 2009). We have developed and rigorously validated a method (Bansal et al., 2005) that measures differences in morphological features as distances between corresponding points across the surfaces of a region within the brains of a group of participants relative to the corresponding region in a template brain, thereby allowing localization of group differences in distances at each voxel on the surface of that brain region. Those differences in distance provide measures of differences in shape that we then interpret as group increases or decreases in local surface volumes within that region.

Few longitudinal studies have attempted to predict the conversion from MCI to AD using hippocampal surface morphology (Csernansky et al., 2005). In 169 patients with MCI who had baseline MRI scans in a 3-year multicenter treatment trial that compared donepezil, vitamin E, and placebo, 3D measures derived from radial atrophy mapping from the hippocampal surface to its medial core correlated with visual ratings of medial temporal lobe atrophy, and greater CA1 and subicular atrophy was associated with conversion to AD (Apostolova et al., 2010). This pattern of shape deformation is consistent with the spatial distribution of neurofibrillary degeneration within the cellular subfields of the hippocampus in patients with pathologically-confirmed AD (Braak et al., 1996, Corder et al., 2000). Within the medial temporal lobe (MTL), the entorhinal cortex rather than the hippocampus appears to be the earliest site of AD pathology and volume loss (Braak et al., 1991, Gomez-Isla et al., 1996). In an autopsy series, mild AD subjects had a 60% reduction in cell count in

layer II and 40% reduction in layer IV of the entorhinal cortex compared to controls (Gomez-Isla et al., 1996). Smaller entorhinal cortex volume in MCI has been shown to be an early predictor of conversion to AD (Devanand et al., 2007) but surface shape deformation in this relatively small structure has not been studied as a predictor of conversion to AD.

Using MRI-based volumetric analyses from a single-site, long-term follow-up study of a cohort of cognitively impaired outpatients without dementia, we previously showed that smaller hippocampal and entorhinal cortex volumes predicted conversion from MCI to AD (Devanand et al., 2007). In the same sample, we evaluated MRI-based geometric representations of morphological surfaces and surface contours in the hippocampus, parahippocampal gyrus and entorhinal cortex and their associations with subsequent conversion from MCI to AD. We hypothesized that reduced local volumes (surface indentations) in the anterior hippocampus and throughout the entorhinal cortex would characterize the MCI patients who converted to AD during follow-up, and that these measures would be superior to the total volumes of the hippocampus and entorhinal cortex.

## METHODS

### Patients with MCI

As described elsewhere (Tabert et al, 2006; Devanand et al, 2008), patients in the age range of 41–85 years who presented for clinical evaluation with subjective memory complaints of at least 6 months' duration to a Memory Disorders Center were eligible for the study if they had a Folstein MMSE (Folstein et al, 1975) score of 22 or greater out of 30 (relatively low cutoff to account for primary Spanish speakers; Siedlecki et al, 2010), and cognitive impairment defined as MMSE recall ≤ 2/3 objects at 5 min or the 12-item 6-trial Selective Reminding Test (SRT) delayed recall score > 1 SD below norms or Wechsler Adult Intelligence Scale-Revised (WAIS-R) performance IQ score > 10 points below WAIS-R verbal IQ score. Patients without these deficits were considered if the informant confirmed memory decline and the modified Blessed Functional Activity Scale score was ≥ 1 on the first 8 items that cover cognitive and functional deficits (Blessed et al, 1968, Stern et al, 1990). Final determination for inclusion was based on a consensus diagnosis between two expert raters (DPD, YS).

This study began before mild cognitive impairment (MCI) criteria were published (Devanand et al., 2008). Baseline MCI subtype was determined post hoc by using age, education, and sex-based regression norms derived from 83 healthy control subjects (Devanand et al., 2008). Using this approach, 73% of patients met criteria for amnestic MCI with or without other cognitive domain deficits. Exclusion criteria were a diagnosis of dementia, schizophrenia, current major affective disorder, alcohol or substance dependence, history of stroke, cortical stroke or infarct ≥ 2 cm in diameter on MRI, cognitive impairment entirely caused by medications, or other major neurological illness. Patients were evaluated every 6 months during follow-up, and a consensus diagnosis was made by the same two expert raters (DPD, YS) at each time point (Devanand et al., 2008). The diagnosis of AD was based on the NINCDS-ADRDA criteria (McKhann et al, 1984).

### Healthy control subjects

Healthy controls (n=61), group matched to patients on age and gender, were recruited primarily by advertisement. Inclusion criteria were the absence of memory complaints, score ≥ 27/30 on the MMSE with recall ≥ 2/3 objects at 5 minutes, and neuropsychological test scores less than one standard deviation below age-adjusted norms. Exclusion criteria were the same as for patients. All participants signed informed consent in this IRB-approved protocol.

### MRI Scan Acquisition

We acquired brain MRI data only at baseline for each participant using a GE 1.5T Signa 5X scanner. T1-weighted sagittal scout images, T1-weighted axial images, and proton density and T2-weighted fast spin echo coronal images were acquired as described elsewhere (Devanand et al., 2007). For volumetric analysis of the medial temporal lobe, a 3D coronal volume spoiled gradient recalled echo (SPGR) sequence was acquired, perpendicular to the temporal horns, with TR=34 ms, TE=13 ms, flip angle=45 degrees, slice thickness=2 mm, slices spacing=0 mm, matrix = 256 × 256, NEX=1, and FOV=24 cm × 18 cm.

### MRI Processing

For morphologic region definition and volumetric analyses, a single rater (G.P.) blind to subject information evaluated all scans on a Sun UltraSPARC workstation, using a dedicated software package (MIDAS) for image segmentation and coregistration (Tsui et al., 2001). This rater trained with expert raters and showed high interrater reliability on 10 scans (sum of left and right volumes): hippocampal volume intraclass correlation coefficient (ICC)=0.90, parahippocampal gyrus volume ICC =0.96, and entorhinal cortex volume ICC=0.92 (Devanand et al., 2007). The rater blindly re-rated 10 scans that she had rated more than a year earlier and showed high intra-rater reliability: hippocampal volume ICC=0.98, parahippocampal gyrus volume ICC=0.97, and entorhinal cortex volume ICC=0.99 (Devanand et al., 2007).

### Volumetric analyses

For the hippocampal volume assessment method, the lateral border of the hippocampus was the medial wall of the temporal horn; the anterior boundary was the amygdala with the transition cortex between the amygdala cortical nucleus and hippocampus excluded by making a perpendicular section at the level of the semilunar gyrus. Anteriorly, the superior border was defined by the temporal horn and fimbria, the medial border by the ambient cistern, and the inferior border by the uncal sulcus and parahippocampal gyrus. More posteriorly, the hippocampal body's medial boundary was the transverse fissure, and its inferior boundary was the parahippocampal gyrus (medial part of the subiculum if the uncal sulcus was not visible). Because the interface between the lateral portion of the subiculum and the hippocampus (Ammon's horn) cannot be distinguished, this portion was included in the hippocampus and not the parahippocampal gyrus.

The parahippocampal gyrus volume included the medial portion of the subiculum, the entorhinal cortex, the transentorhinal cortex, and the parahippocampal neocortex and white matter. The medial border was the ambient cistern, and the inferior border was the tentorium cerebelli. In anterior sections, the superior border of the parahippocampal gyrus was the hippocampus and the uncal sulcus. In more posterior sections, the superior boundary was the hippocampus laterally and the transverse fissure. The medial part of the subiculum (presubiculum and parasubiculum) was included in the parahippocampal gyrus volume. The anterior and posterior boundaries of the parahippocampal gyrus corresponded to the same level (slice) as the anterior and posterior boundaries of the hippocampus. This approach standardized the procedures across all subjects but may have led to exclusion of the anterior-most and posterior-most portions of both structures.

The entorhinal cortex was assessed by estimating the volume across three slices according to the method validated by Killiany et al. (2002). First, the mammillary bodies were identified. The first (most rostral) image displaying the fornix white matter tracts was the center image, and the adjacent anterior and posterior slices were then identified. The outline began at the angle formed by the junction of the rhinal sulcus and the brain surface and then transected the angle formed by the rhinal sulcus and the inferomedial brain surface. The line cut across

the gray matter and then followed the lower edge of the white matter to the inferior hippocampal surface and down along the brain surface to the initial outline point. The outlines used the same landmarks on all three slices.

## Surface Morphometry

We applied procedures for surface morphometry, previously developed and validated using both synthetic and real-world datasets (Bansal et al., 2005) for detailed analysis of local volumes across the entire surface of the template hippocampus, entorhinal cortex, and parahippocampal gyrus. The template brain regions were selected using a rigorous, two-step procedure such that the brain regions were morphologically the most representative (in the least squares sense) of the brain regions in our cohort of healthy participants (Plessen et al., 2006). The brains for all participants were coregistered to the template brain using a similarity transformation (3 translations, 3 rotations, and global scaling) that maximized mutual information in grayscale values (Bansal et al., 2005, Peterson et al., 2007). These parameters were applied to adjust for overall brain size and to transform the manually defined hippocampus, parahippocampal gyrus and entorhinal cortex volumes (Devanand et al., 2007) into the common template space. The transformed hippocampus, parahippocampal gyrus, and entorhinal cortex of each participant were first individually and rigidly coregistered to the corresponding template structures and then non-linearly warped using a high-dimensional, non-rigid warping algorithm based on fluid flow dynamics (Bansal et al., 2007). The warped hippocampus, parahippocampal gyrus and entorhinal cortex were then unwarped into the template space for each structure present before the high-dimensional warp was applied, while maintaining the labels for corresponding points on the surfaces of the participant and template structures, thereby allowing computation of Euclidean distances between corresponding points across the surface of a participant's structure and the surface of the template structures. These distances were labeled positive for outward deformations and negative for inward deformations in each participant's structure as compared to the template structure. These distances were rescaled by intracranial volume (ICV) to control for variability in and across participants.

## Statistics

ANOVA, ANCOVA and $\chi^2$ test were used to compare the demographic, clinical and MRI variables of patients (converters, non-converters to AD) and controls. Student's t-test was used for two group comparisons (MCI and controls) of relevant variables.

Signed euclidean distances from the template at each voxel on the surface of each region were compared statistically between groups using linear regression. Separate analyses were conducted for left and right hippocampus, entorhinal cortex, and parahippocampal gyrus. For each comparison, age, sex, education and intracranial volume were covariates, with the additional covariates of baseline MMSE or SRT total immediate recall or SRT delayed recall in specific analyses. The two SRT measures were chosen *a priori* from the neuropsychological test battery because episodic verbal memory deficits characterize mild AD and these measures were strong predictors of conversion in this sample as reported previously (Tabert et al., 2006). False discovery rate (FDR) correction for multiple comparisons was used for all analyses.

The initial analyses compared the MCI and control groups. Within the MCI sample, voxel-wise analyses of prediction of conversion to AD first used Cox regression (survival analysis) for the entire follow-up duration and then logistic regression for the 3-year follow-up sample. The 3-year duration was chosen because most conversions are known to occur within this time frame (Petersen, 2007) and to evaluate clinically relevant short-term to

intermediate-term conversion to AD. For early converters to AD who did not reach 3-year follow-up, the diagnosis was assumed to have remained AD.

# RESULTS

## Demographic and Clinical Features

Among subjects who had MRI scans, 130 of 140 patients with MCI and 61 of 63 controls (excluding one control used for the reference template) had imaging data of sufficient quality, after coregistration, to delineate the hippocampus and parahippocampal gyrus using surface morphometry. For entorhinal cortex, 124 patients and 60 controls provided data of adequate quality for surface morphometry.

MCI converters, MCI non-converters, and controls did not differ in gender distribution, or apolipoprotein E ε4 carrier status (Table 1). MCI converters (n=31) were older, had lower education, and scored lower on baseline MMSE than MCI non-converters (n=99) or controls (n=61) (Table 1). The features of the amnestic MCI group (n=94) that included converters and non-converters are displayed in Table 1. There were 5 subjects with MCI who were rated as “normal” during follow-up and they were included among the non-converters. Two control participants cognitively declined and met criteria for amnestic MCI during follow-up, and none converted to AD.

## MCI-Control comparison

Baseline analyses were conducted separately for the left and right hippocampus, entorhinal cortex, and parahippocampal gyrus, with participant group (MCI or control) and sex as between subject factors and age and education in years as covariates. The hippocampal subregions are displayed in Figure 1 and the MCI-control comparisons using the surface projections are displayed in Figure 2. In the hippocampus, patients with MCI showed reduced local volumes compared to controls in the dorsal and dorso-anterior portions of the head and body that were more prominent in the left hippocampus. The differences were localized predominantly to the left cornu ammonis (CA) region ($p < .0001$) and to a lesser extent the left subiculum and hippocampal-amygdaloid transitional area ($P < .025$). In the entorhinal cortex, patients with MCI showed widespread reduced local volumes bilaterally compared to controls in several regions, but particularly in the mediodorsal portions of this structure ($P$’s $< .025$ to $.0001$). In the parahippocampal gyrus, patients with MCI showed reduced local volumes bilaterally compared to controls predominantly in the mid-dorsal and mid-ventral regions ($p < .025$ to $p < .0001$).

## Survival analyses

In the MCI sample, Cox regression models were conducted at each point on the surface of these structures for the time to conversion for converters to AD (n=31) and non-converters (n=99, right-censored observations). As displayed in Figure 3, converters at baseline showed pronounced reductions in local volumes compared to non-converters in the anterior CA region bilaterally (head of the hippocampus; $p$’s $< .025$ to $.0001$), an adjacent portion of the subiculum ($p < .025$) and the dentate gyrus ($p < .025$). In the entorhinal cortex, several regions were reduced in local volumes in converters to AD that were most prominent in the anterior-inferior pole bilaterally. In the parahippocampal gyrus, the effects were less robust and prominent in the mid-regions in the dorso-anterior and dorsal projections bilaterally ($p < .025$). Results were similar in additional Cox analyses that also covaried for MMSE or SRT total immediate recall or SRT delayed recall (Figure 3).

For the left and right hippocampus and entorhinal cortices, individual points were identified visually from the center of the most prominently significant clusters of points of inward

deformation. The distance of each point from the corresponding point in the template brain, and the volume of the relevant structure (left or right hippocampus or entorhinal cortex) were both included in the same Cox regression model with age, sex, education and intracranial volume. In these analyses, the distances of the points chosen in the CA1 region in the right hippocampus, subiculum in the right hippocampus, subiculum in the left hippocampus, and anterior inferiomedial points in the right and left entorhinal cortex, remained highly significant whereas the volumes of the left/right hippocampus/entorhinal cortex in which the points were located were either marginally significant or not significant. The hazard ratios and 95% confidence intervals are displayed in Table 2.

Whereas survival analyses identified several regions of reduced local volume at baseline, indicating a localized reduction in tissue, several regions of increased local volumes were also detected. In MCI converters compared to non-converters, these included the left parasubiculum ($p = .0001$) and CA3 bilaterally and a portion of the tail of the hippocampus ($p=.025$), and the right ventroposterior ($p=.025$) and left medial regions ($p=0.025$ to $0.001$) of the entorhinal cortex (Figure 3). For the parahippocampal gyrus, a suggestion of increased volumes was present in the anterodorsal and ventromedial regions ($p = .025$, Figure 3).

### Logistic regression analyses in the 3-year follow-up MCI sample

Statistical maps as displayed in Figure 4 (supplemental figure) show that at baseline, MCI converters had pronounced reductions in local volumes as compared to non-converters in (1) the hippocampal CA region bilaterally ($p < .0001$) and (2) the dentate gyrus and subiculum ($p < .025$). The subregions involved in the hippocampus and parahippocampal gyrus were similar in the survival and logistic regression analyses. Entorhinal cortex showed reduced local volumes predominantly in the anterior pole and mid-region in converters compared to non-converters at baseline. This set of findings was largely sustained with slight variation in regions of local volume reductions after covarying for MMSE or SRT total recall or SRT delayed recall in each of these logistic regression models (Figure 4). When apolipoprotein E ε4 genotype was included as a covariate the findings did not change appreciably. Further, when the sample was restricted to patients who met the Petersen criteria for amnestic MCI, the findings were similar to those obtained in the entire sample.

## DISCUSSION

Surface morphometry analyses showed inward deformation, interpreted as highly localized volume reductions, in specific medial temporal lobe regions in patients with MCI compared to controls. Within the MCI group, reductions in local volumes at baseline in specific regions of the hippocampus and entorhinal cortex, and to a lesser degree in the parahippocampal gyrus, were strongly associated with conversion to AD, even after controlling for demographic and cognitive measures (Devanand et al., 2008). These findings did not depend on apolipoprotein E genotype, and remained strong when the sample was restricted to amnestic MCI (Petersen et al., 2001). When the distance of each point from the corresponding point in the template brain, and the volume of the corresponding anatomical structure, were both included in the same Cox regression model, the distances representing inward deformation remained highly significant whereas the volumes (left/right hippocampus/entorhinal cortex) were either marginally significant or not significant. These results show that the surface morphometry method may be a stronger predictor of conversion to AD than hippocampal or entorhinal cortex volumes. Of note, increases in local volumes were not prominent in the comparison of MCI converters to non-converters and only one measure was highly significant, suggesting that localized increases in volume in medial temporal regions typically do not characterize converters to AD.

In the hippocampus, the greatest differences between MCI converters and non-converters were concentrated in the cornu ammonis (CA1/CA3) subfield and the subiculum in the anterior hippocampus. In a study of 49 non-demented elderly men and women followed for approximately 5 years, localized atrophy in the lateral zone of the left hippocampus corresponding to the CA1 subfield was the strongest predictor of conversion to a Clinical Dementia Rating (CDR) of 0.5 that overlaps closely with MCI and minimal AD (Csernansky et al., 2005). In the clinical trial that compared donepezil, vitamin E, and placebo in patients with MCI with 3-year follow-up, reductions in local volumes in the CA1 and subiculum regions were associated with conversion to AD during 3-year follow-up (Apostolova et al., 2010). In that study, localized volume reduction was more prominent in the right than left hippocampus, which contrasts to some extent with our study and some of the literature (Csernansky et al., 2005).

During the course of AD, the regionally-specific shape effects in the hippocampus appear to start anteriorly in the CA1 and subiculum regions, then propagate to the CA2 and CA3 regions (Apostolova et al., 2006, Wang et al., 2006, Wang et al., 2009). Our findings are consistent with this model. The anterior hippocampus is involved in novelty detection (Daselaar et al., 2006), and it encodes the spatial and temporal relationships between sensory experiences (Agster et al., 2002, Bast et al.,2003), which the posterior hippocampus then consolidates for storage in long-term memory (Strange et al.,1999). The CA1, CA2 and CA3 subregions differentially contribute to successful encoding based on event content, and the subiculum may contribute to successful encoding irrespective of event content (Preston et al., 2010). The CA1 region supports intermediate episodic memory and processes of temporal pattern separation processes that reduce interference among sequentially experienced items. These processes can require CA1 involvement even in short-term episodic tasks based on duration (Kesner et al., 2010). The subiculum is primarily involved in communicating information from the hippocampus to several other brain regions, and damage to this region may be linked to the difficulties that patients with incipient AD have with associative memories and related cognitive tasks. Our findings at the MCI stage in converters to AD of greater anterior hippocampal inward deformation, particularly in the CA1 and subiculum regions, are consistent with the clinical features of very mild AD.

Neuropathology shows neuronal loss specific to layers II and IV in the hippocampus in early AD (Gomez-Isla et al., 1996, Hyman et al., 1984). The affected cells in these layers connect the hippocampus with association cortices, thalamus, hypothalamus and basal forebrain, and their damage is believed to cause early memory impairment in the disease (Hyman et al., 1984). Dynamic patterns of gray-matter loss occur in AD patients who average gray-matter losses of nearly 5% per year in contrast to 1% per year in healthy controls (Barnes et al., 2004, Thompson et al., 2003). Neuropathological studies show that neuronal loss in the CA1 and subiculum regions is associated with AD or grades of cognitive impairment in AD (Corder et al., 2000, Thompson et al., 2003).

Inward surface deformation in several portions of the entorhinal cortex, particularly the anterior-inferior pole, showed significant associations with conversion from MCI to AD. Surface deformation of the entorhinal cortex has not been examined previously as a predictor of MCI conversion to AD, but our novel findings are broadly consistent with the results obtained from volumetric analysis in this same sample (Devanand et al., 2007). The entorhinal cortex is one of the earliest structures demonstrating neurofibrillary tangles in early AD (Gomez-Isla et al., 1996) and the MRI findings of atrophy in various portions of the entorhinal cortex are consistent with established neuropathological findings.

Atrophy of the parahippocampal gyrus was also associated with conversion from MCI to AD, but with less robust effects (Pantel et al., 2003). One possible explanation is that the

parahippocampal gyrus is relatively large, and regions other than its component entorhinal cortex, which makes up a very small fraction of the structure, may not be severely affected at the MCI stage in converters to AD. Our previous results from volumetric analyses in this same sample support this view (Devanand et al., 2007). Volumes of the parahippocampal gyrus included white matter, and the degree to which tissue loss in early AD extends into the white matter is uncertain (Thompson et al, 2003, Rusinek et al., 1991).

This study has several limitations. First, its results can be applied only to outpatients presenting for evaluation of memory complaints, and not to the general population. To improve clinical relevance, the inclusion/exclusion criteria broadly identified cognitively impaired patients without dementia, though most met criteria for amnestic MCI and the main findings held in this large subsample. Second, the primary outcome of AD was based on clinical diagnosis, not neuropathology, and this may have led to classification error, though expert raters employed strict diagnostic methods. Third, MCI converters were older and less educated than non-converters and healthy controls. These factors were included as linear covariates, but non-linear effects of these variables could have persisted in the analyses. Fourth, the ultrastructural determinants of group differences in morphology of medial temporal lobe structures are unknown, as is the extent to which disturbances in surface morphology relate to abnormalities in the underlying nuclei within these structures. Fifth, the MRIs were cross-sectional, and hence within-subject trajectories of change in surface morphological features could not be assessed. Finally, the multiple statistical tests performed in our analyses increased the likelihood of type I error, which we minimized in our surface-based analyses through the use of conservative statistical thresholds and FDR-based corrections for multiple comparisons. Overall, our findings support the view that fine-grained analysis of the surface area in medial temporal lobe structures, which takes into account the surface inward and outward deformations that are characteristic of these structures, may enhance our ability to identify incipient AD in patients clinically diagnosed with MCI.

## Supplementary Material

Refer to Web version on PubMed Central for supplementary material.

## Acknowledgments

Supported in part by grants AG17761 and P30 AG08051 from the National Institute of Aging.

## References

1. Agster, et al. The hippocampus and disambiguation of overlapping sequences. J Neurosci. 2002; 22:5760–5768. [PubMed: 12097529]
2. Apostolova, et al. Conversion of mild cognitive impairment to Alzheimer disease predicted by hippocampal atrophy maps. Arch Neurol. 2006; 63(5):693–699. [PubMed: 16682538]
3. Apostolova, et al. 3D comparison of low, intermediate, and advanced hippocampal atrophy in MCI. Hum Brain Mapp. 2010; 31:786–797. [PubMed: 20143386]
4. Bansal, et al. ROC-based assessments of 3D cortical surface-matching algorithms. Neuroimage. 2005; 24(1):150–162. [PubMed: 15588606]
5. Bansal, et al. Statistical analyses of brain surfaces using Gaussian random fields on 2-D manifolds. IEEE Trans Med Imaging. 2007 Jan; 26(1):46–57. [PubMed: 17243583]
6. Barnes, et al. Differentiating AD from aging using semiautomated measurement of hippocampal atrophy. Neuroimage. 2004; 23:574–581. [PubMed: 15488407]
7. Bast, Feldon. Hippocampal modulation of sensorimotor processes. Prog Neurobiol. 2003; 70:319–345. [PubMed: 12963091]

8. Blessed, et al. The association between quantitative measures of dementia and of senile change in the cerebral grey matter of elderly subjects. Br J Psychiatry. 1968; 114:797–811. [PubMed: 5662937]
9. Braak H, Braak E. Neuropathological staging of Alzheimer-related changes. Acta Neuropathol (Berl). 1991; 82:239–259. [PubMed: 1759558]
10. Braak H, Braak E. Development of Alzheimer-related neurofibrillary changes in the neocortex inversely recapitulates cortical myelogenesis. Acta Neuropathol. 1996 Aug; 92(2):197–201. [PubMed: 8841666]
11. Burggren, et al. Reduced cortical thickness in hippocampal subregions among cognitively normal apolipoprotein E e4 carriers. Neuroimage. 2008; 41(4):1177–1183. [PubMed: 18486492]
12. Corder, et al. Density profiles of Alzheimer disease regional brain pathology for the Huddinge brain bank: pattern recognition emulates and expands upon Braak staging. Exp Gerontol. 2000; 35:851–864. [PubMed: 11053676]
13. Csernansky, et al. Preclinical detection of Alzheimer's disease: hippocampal shape and volume predict dementia onset in the elderly. Neuroimage. 2005 Apr 15; 25(3):783–792. [PubMed: 15808979]
14. Daselaar, et al. Triple dissociation in the medial temporal lobes: recollection, familiarity, and novelty. J Neurophysiol. 2006; 96(4):1902–1911. [PubMed: 16738210]
15. de Leon, et al. MRI and CSF studies in the early diagnosis of Alzheimer disease. J Intern Med. 2004; 256:205–223. [PubMed: 15324364]
16. De Santi, et al. Hippocampal formation glucose metabolism and volume losses in MCI and AD. Neurobiol Aging. 2001; 22:529–539. [PubMed: 11445252]
17. Devanand, et al. Hippocampal and entorhinal atrophy in mild cognitive impairment: prediction of Alzheimer disease. Neurology. 2007; 68(11):828–836. [PubMed: 17353470]
18. Devanand, et al. Combining early markers strongly predicts conversion from mild cognitive impairment to Alzheimer's disease. Biol Psychiatry. 2008; 64(10):871–879. [PubMed: 18723162]
19. Folstein, et al. "Mini-mental state". A practical method for grading the cognitive state of patients for the clinician. J Psychiatr Res. 1975; 12:189–198. [PubMed: 1202204]
20. Gomez-Isla, et al. Profound loss of layer II entorhinal cortex neurons occurs in very mild Alzheimer's disease. J Neurosci. 1996; 16:4491–4500. [PubMed: 8699259]
21. Hyman, et al. Alzheimer's disease: cell-specific pathology isolates the hippocampal formation. Science. 1984; 225(4667):1168–1170. [PubMed: 6474172]
22. Jack, et al. Hypothetical model of dynamic biomarkers of the Alzheimer's pathological cascade. Lancet Neurol. 2010; 9:119–128. [PubMed: 20083042]
23. Kesner, Hunsaker. The temporal attributes of episodic memory. Behav Brain Res. 2010 Dec 31; 215(2):299–309. [PubMed: 20036694]
24. Killiany, et al. MRI measures of entorhinal cortex vs hippocampus in preclinical AD. Neurology. 2002; 58:1188–1196. [PubMed: 11971085]
25. Kim, et al. Asymmetry analysis of deformable hippocampal model using the principal component in schizophrenia. Human Brain Mapping. 2005; 25(4):361–369. [PubMed: 15852383]
26. McKhann, et al. Clinical diagnosis of Alzheimer's disease: NINCDS-ADRDA work group. Neurology. 1984; 34:939–944. [PubMed: 6610841]
27. Pantel, et al. Parahippocampal volume deficits in subjects with aging-associated cognitive decline. Am J Psychiatry. 2003; 160:379–382. [PubMed: 12562591]
28. Petersen, et al. Practice parameter: early detection of dementia: mild cognitive impairment (an evidence-based review). Report of the Quality Standards Subcommittee of the American Academy of Neurology. Neurology. 2001; 56:1133–1142. [PubMed: 11342677]
29. Petersen. Mild cognitive impairment: Current research and clinical implications. Semin Neurol. 2007; 27:22–31. [PubMed: 17226738]
30. Peterson, et al. Morphologic features of the amygdala and hippocampus in children and adults with Tourette syndrome. Arch Gen Psychiatry. 2007; 64(11):1281–1291. [PubMed: 17984397]

31. Peterson. Form determines function: new methods for identifying the neuroanatomical loci of circuit-based disturbances in childhood disorders. J Am Acad Child Adolesc Psychiatry. 2010 Jun; 49(6):533–538. [PubMed: 20494263]
32. Plessen KJ, Bansal R, Zhu H, Whiteman R, Amat J, Quackenbush GA, Martin L, Durkin K, Blair C, Royal J, Hugdahl K, Peterson BS. Hippocampus and amygdala morphology in attention-deficit/hyperactivity disorder. Arch Gen Psychiatry. 2006; 63(7):795–807. [PubMed: 16818869]
33. Preston, et al. High-resolution fMRI of content-sensitive subsequent memory responses in human medial temporal lobe. J Cogn Neurosci. 2010 Jan; 22(1):156–173. [PubMed: 19199423]
34. Qiu, et al. Alzheimer's Disease Neuroimaging Initiative. Regional shape abnormalities in mild cognitive impairment and Alzheimer's disease. Neuroimage. 2009; 45(3):656–661. [PubMed: 19280688]
35. Rusinek, et al. Alzheimer Disease: measuring loss of cerebral gray matter with MR imaging. Radiology. 1991; 178:109–114. [PubMed: 1984287]
36. Siedlecki, et al. Do neuropsychological tests have the same meaning in Spanish speakers as they do in English speakers? Neuropsychology. 2010 May; 24(3):402–411. [PubMed: 20438217]
37. Stern, et al. Measurement and prediction of functional capacity in Alzheimer's disease. Neurology. 1990; 40:8–14. [PubMed: 2296387]
38. Stoub, et al. MRI predictors of risk of incident Alzheimer disease: a longitudinal study. Neurology. 2005; 64:1520–1524. [PubMed: 15883311]
39. Strange B, Dolan R. Functional segregation within the human hippocampus. Mol Psychiatry. 1999; 4:508–511. [PubMed: 10578231]
40. Styner, et al. Statistical Shape Analysis of Brain Structures using SPHARM-PDM. Insight Journal DSpace. 2006
41. Tabert, et al. Neuropsychological Prediction of Conversion to Alzheimer's Disease in Patients with Mild Cognitive Impairment. Arch Gen Psychiatry. 2006; 63:916–924. [PubMed: 16894068]
42. Tepest, et al. Hippocampal surface analysis in subjective memory impairment, mild cognitive impairment and Alzheimer's dementia. Dement Geriatr Cogn Disord. 2008; 26(4):323–329. [PubMed: 18841017]
43. Thompson, et al. Dynamics of gray matter loss in Alzheimer's disease. J Neurosci. 2003; 23:994–1005. [PubMed: 12574429]
44. Tsui, et al. Analyzing multi-modality tomographic images and associated regions of interest with MIDAS. SPIE Medical Imaging: Image Processing. 2001; 4322:1725–1734.
45. Wang, et al. Abnormalities of hippocampal surface structure in very mild dementia of the Alzheimer type. Neuroimage. 2006 Mar; 30(1):52–60. [PubMed: 16243546]
46. Wang, et al. Fully-automated, multi-stage hippocampus mapping in very mild Alzheimer disease. Hippocampus. 2009; 19(6):541–548. [PubMed: 19405129]

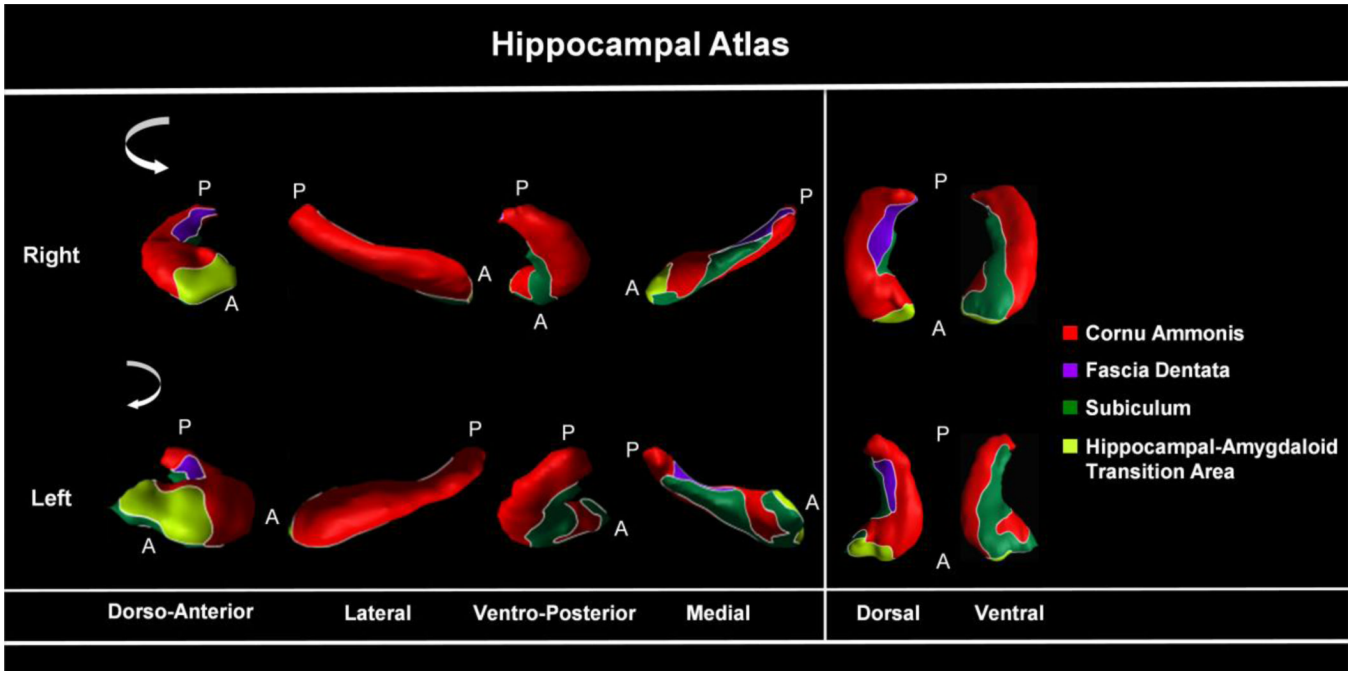


**Figure 1.**

Cytoarchitectonic atlas of Hippocampal Subregions:. the external morphologic projections of the four hippocampal subregions: RED = Cornu Ammonis, GREEN = subiculum, PURPLE = dentate gyrus, LIME GREEN = Hippocampal Amygdaloid transitional area. Only hippocampal subregions have been defined, not subregions of the entorhinal cortex or parahippocampal gyrus.

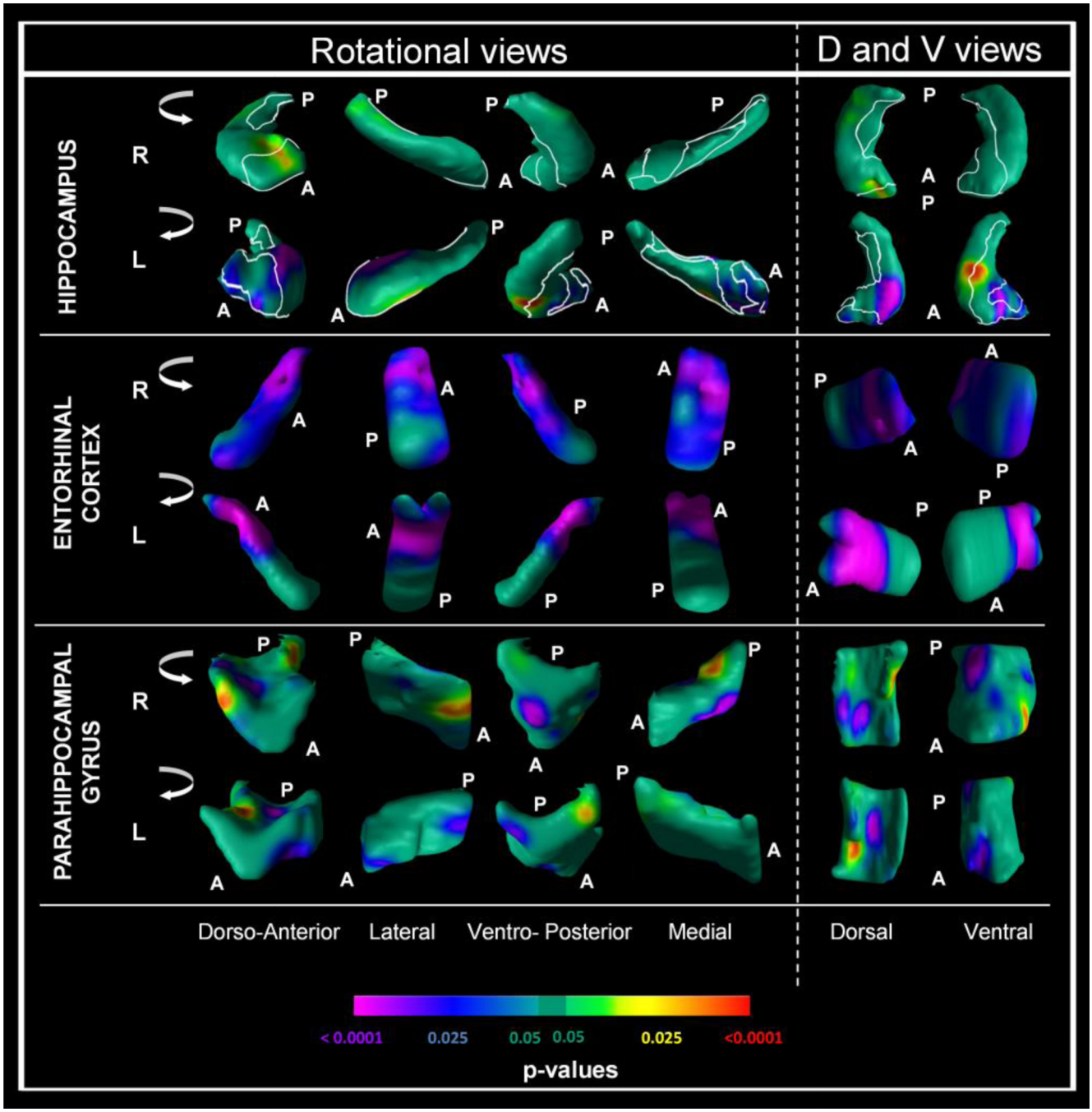


**Figure 2.**

Comparison of 130 patients with mild cognitive impairment (MCI) and 61 normal controls. Analyses conducted at each point on the surface of the hippocampus, entorhinal cortex and parahippocampal gyrus, controlling for age, sex, education and intracranial volume. The right (R) and left (L) Hippocampus, right (R) and left (L) Entorhinal Cortex and the right (R) and left (L) Parahippocampal Gyrus are shown in shown in rotating views and in their dorsal (D) and ventral (V) orientations. All images reflect false discovery rate (FDR) correction for multiple statistical comparisons. The color bar indicates the color coding for P values associated with the main effect of diagnosis (MCI versus controls), with warmer colors (yellow and red) indicating protruding surfaces, presumably from larger underlying

volumes, and cooler colors (blue and purple) indicating indented surfaces presumably from smaller underlying volumes in those locations.

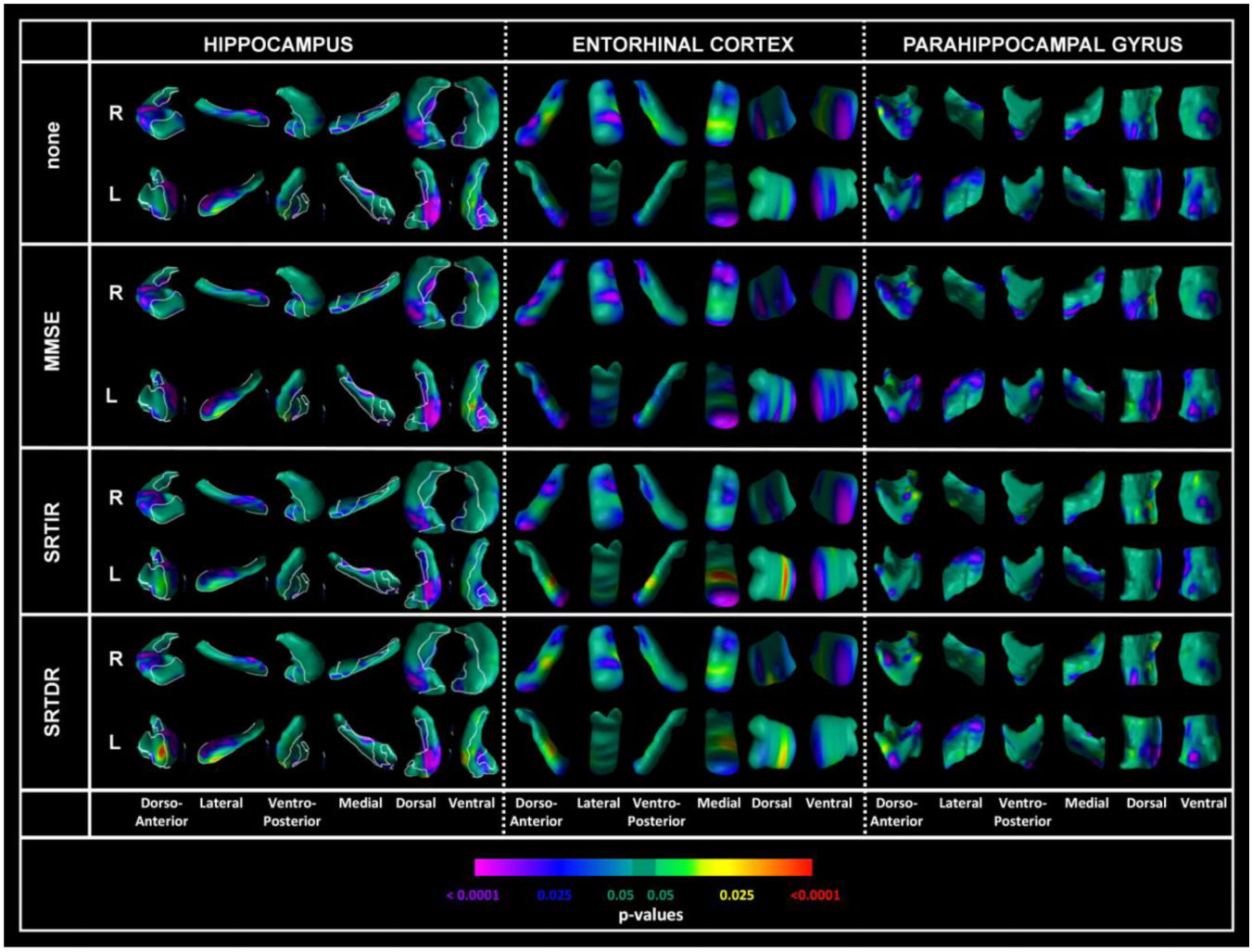


**Figure 3.**

Survival analyses in the MCI sample (n=130; 31 converters and 99 nonconverters). Survival analysis in the MCI sample, conducted at each point on the surface of (R) and left (L) Hippocampus, right (R) and left (L) Entorhinal Cortex and the right (R) and left (L) Parahippocampal Gyrus. All analyses controlled for age, sex, education, and intracranial volume. All images reflect false discovery rate (FDR) correction for multiple statistical comparisons. Cox regression (survival analysis) was conducted for the time to conversion to Alzheimer's disease (AD, right-censored observations). Additional analyses also included total MMSE score (MMSE), SRT total immediate recall (SRTIR), or SRT delayed recall (SRTDR) as a covariate. Color bar coding and orientations and rotation views are the same as in Figure 2.

**Table 1**

Baseline features of patients with MCI (converters and non-converters to AD) and healthy control participants.

| Feature | Patients with MCI | | Healthy Controls | *P< | Amnestic MCI |
|---|---|---|---|---|---|
| | 31 Converters | 99 Non-converters | 61 controls | | 94 patients |
| Gender % female | 56.8 | 55.6 | 54.8 | .99 | 55.3 |
| Baseline Age in years, mean ±SD | 73.2 ± 7.0 | 65.2 ± 10 | 66.2 ± 9.3 | .001 | 67.7 ± 9.5 |
| Education in years, mean ±SD | 13.7 ± 5.0 | 15.3 ± 4.2 | 16.7 ± 2.6 | .002 | 14 ± 5 |
| Baseline MMSE, mean ± SD | 26.3 ± 2.2 | 28.0 ± 2.0 | 29.3 ± 0.8 | .0001 | 27.0 ± 2 |
| Apolipoprotein E ε4 carrier % | 39 | 24 | 21 | .18 | 0 ± 1 |
| +Follow-up duration in years | 2.2 ± 1.7 | 4.68 ± 2.37 | 5.34 ± 2.50 | .001 | 3.91 ± 2.58 |
| **Hippocampal volume (R+L) | 3.75 ± 0.72 | 4.40 ± 0.57 | 4.35 ± 0.56 | .001 | 4.15 ± 0.60 |
| **Parahippocampal gyrus volume (R+L) | 5.80 ± 1.17 | 6.67 ± 0.94 | 6.70 ± 1.0 | .001 | 6.31 ± 1.06 |
| **Entorhinal cortex volume (R+L) | 0.37 ± 0.08 | 0.46 ± 0.08 | 0.55 ± 0.10 | .001 | 0.44 ± 0.09 |
| Supratentorial intracranial volume in cc | 1287 ± 117 | 1306 ± 127 | 1316 ± 131 | .57 | 1294 ± 127 |

All values are means ± standard deviations, or percentages.
MMSE: 30-item Folstein Mini-Mental State Exam.

*P: P value in ANOVA and ANCOVA comparison of MCI converters, non-converters, and healthy controls.

+Converters to AD exited the study after 2 consecutive annual AD diagnoses, thereby reducing the follow-up duration in this group.

*Significance level for $\chi^2$ or ANOVA (ANCOVA for hippocampal, parahippocampal gyrus and entorhinal cortex volumes, covarying for age, education and intracranial volume).

**Hippocampal, parahippocampal gyrus and entorhinal cortex volumes are in cubic cm. In ANCOVAs, hippocampal and parahippocampal gyrus and entorhinal cortex volumes were analyzed for converters/non-converters/controls restricted to the 3-year follow-up sample, covarying for intracranial volume.

**Table 2**

Cox regression (survival) analyses of conversion from mild cognitive impairment to Alzheimer's disease (31 converters, 99 non-converters). Individual points were identified visually from the center of the most prominently significant clusters of points of inward deformation. The distance of each point from the corresponding point in the template brain, and the volume of the structure (left or right hippocampus or entorhinal cortex) were both included in the same Cox regression model with age, sex, education and intracranial volume. Each Cox regression model is represented in one row with only two variables shown: distance of the point from the corresponding point on the template brain, and the volume of the relevant anatomical structure in which the point was located.

| Location | Distance of Point | | | Volume | | |
|---|---|---|---|---|---|---|
| | Hazard ratio | 95% CI | P = | Hazard ratio | 95% CI | P = |
| CA1, right hippocampus | 0.472 | 0.258, 0.861 | 0.01 | 0.224 | 0.049, 1.028 | 0.054 |
| CA1, left hippocampus | 0.821 | 0.608, 1.108 | 0.20 | 0.226 | 0.048, 1.055 | 0.06 |
| Subiculum, right hippocampus | 0.472 | 0.258, 0.861 | 0.01 | 0.224 | 0.049, 1.028 | 0.054 |
| Subiculum, left hippocampus | 0.229 | 0.108, 0.486 | 0.0001 | 0.219 | 0.057, 0.845 | 0.03 |
| Entorhinal cortex, right anterior inferiomedial | 0.350 | 0.201, 0.609 | 0.0002 | 0.054 | 0.00, 52.08 | 0.06 |
| Entorhinal cortex, left anterior inferiomedial | 0.518 | 0.353, 0.760 | 0.0008 | 0.016 | 0.00, 19.68 | 0.26 |